HEFAT2014
10th International Conference on Heat Transfer, Fluid Mechanics and Thermodynamics
14 – 16 July 2014
Orlando, Florida

NON-SIMILAR SOLUTION FOR MIXED CONVECTION IN A POROUS MEDIUM SATURATED WITH NANOFLUID

Srinivasacharya D.* and Surender O.
*Author for correspondence
Department of Mathematics,
National Institute of Technology Warangal,
Andhra Pradesh, 506004,
India.
E-mail: dsc@nitw.ac.in, surenderontela@nitw.ac.in

ABSTRACT

This article explores the analysis of mixed convection boundary layer flow over a vertical flat plate embedded in a porous medium saturated by a nanofluid in the presence of radiation effect. The vertical plate is maintained at uniform and constant heat, mass and nanoparticle fluxes. The Darcy model is considered to describe the flow in the porous medium. The effects of Brownian motion and thermophoresis are incorporated in to the model for nanofluids. In addition, the thermal energy equations include regular diffusion and cross-diffusion terms. A suitable coordinate transformation is introduced, and the resulting system of non-similar, coupled and nonlinear partial differential equations is solved numerically by using implicit finite difference method. A comparison is made with the available results in the literature, and our results are found to be in very good agreement. The influence of pertinent parameters on the non-dimensional velocity, temperature, concentration and nanoparticle volume fraction are discussed. In addition, the variation of heat, mass and nanoparticle transfer rates at the plate are exhibited graphically for different values of physical parameters.

NOMENCLATURE

B	Regular buoyancy parameter
C	Concentration
Da	Darcy parameter ($=K_p/L^2$)
D_B	Brownian motion diffusion coefficient
D_{CT}	Soret type diffusivity
D_s	Mass diffusivity
D_T	Thermophoretic diffusion coefficient
D_{TC}	Dufour type diffusivity
f	Dimensionless stream function
g^*	Acceleration due to gravity
g	Dimensionless nanoparticle fraction
Gr	Grashof number
k	Thermal conductivity
k^*	Mean absorption coefficient
K_p	Permeability
L_d	Dufour-solutal Lewis number
N_b	Brownian motion Parameter
N_d	Modified Dufour number
N_r	Nanofluid buoyancy parameter
N_t	Thermophoresis parameter
Nu_ξ	Non-dimensional Nusselt number
Pr	Prandtl number ($=\nu/\alpha$)
q_r	Radiative heat flux
R	Radiation parameter
s	Dimensionless concentration
Sc	Schmidt number (¼ m=Ds)
Sc_n	Nanoparticle Schmidt number ($=\nu/D_B$)
$Sh_{n,\xi}$	Non-dimensional Sherwood number
T	Temperature
u, v	Velocity components in the x- and y-directions respectively.
x, y	Cartesian coordinates along the plate and normal to it

Greek symbols

β_T	Coefficient of thermal expansion
β_C	Coefficient of concentration expansion
ρ_p	Density of nanoparticles
ρ_f	Density of the base fluid
θ	Dimensionless temperature
ν	Kinematic viscosity
ϕ	Nanoparticle volume fraction
ξ	Non-similarity variable
η	Similarity variable
ψ	Stream function
α	Thermal diffusivity
σ^*	Stefan-Boltzmann constant
μ	Viscosity of the fluid

Subscripts

W	Condition at wall
∞	Condition at infinity

Superscript

‘	Differentiation with respect to η

INTRODUCTION

The study of nanofluids has allured extensive interest from research in view of their notable applications to electronics, optical devices, communication, high-power X-rays, computing technologies, scientific measurement, lasers, material processing, medicine and material synthesis. The idea of using

nanofluids is to enhance heat transfer due to their anomalously high thermal conductivity. For instance, consider the radiator of a vehicle. Using nanofluids as coolants would allow for the radiators with compact sizes and better positioning, this leads to an elegant and efficient design of a vehicle. Besides, Nanofluids are used for cooling of microchips in computers, other electronics and many more which use microfluidic applications Nanofluids are prepared by dispersing solid nanoparticles in conventional fluids such as water, oil or ethylene glycol. It is shown that the addition of a small amount of nanometre sized (less than 1 by volume) particles to conventional heat transfer liquids enhanced the thermal conductivity of the fluid [1]. The detailed introduction and applications of nanofluids is given in the book [2]. The factors which contribute to abnormal thermal conductivity increase relative to base fluids and viscosity have been investigated [3]. He developed an analytical model for convective transport in nanofluids, which incorporates the effects of Brownian motion and thermophoresis. The random motion of nanoparticles within the base fluid is said to be Brownian motion, and this results from continuous collisions between the nanoparticles and the molecules of the base fluid. Particles can diffuse under the effect of a temperature gradient. This phenomenon is called thermophoresis, and is the particle equivalent of the well-known Soret effect for gaseous or liquid mixtures. The literature on nanofluids has been reviewed by some authors [4, 5]. These reviews examine in detail the work done on convective transport in nanofluids.

The study of convective flow, heat transfer in porous media has been the subject of enormous importance and interest in the recent years owing to its extensive applications, such as thermal insulation, extraction of crude oil and chemical catalytic reactors etc. The process of heat and mass transfer induced by the simultaneous effect of natural and forced convection is called mixed convection flow. Considerable attention has been paid to the theoretical and numerical investigation of mixed convection boundary layer flow past a vertical plate in the recent years owing to its diverse applications, such as electronic devices cooled by fans, thermal insulation, nuclear reactors cooled during an emergency shutdown, water movement in geothermal reservoirs, solid-matrix compact heat exchangers, solar collectors, energy storage units, ceramic processing, packed bed chemical reactors etc. Considerable studies on mixed convection heat and mass transfer from different geometries have been tackled by various authors. Similarity solutions have been presented for the boundary-layer flow of a nanofluid on a linearly moving permeable vertical surface in the presence of magnetic field, heat generation or absorption, thermophoresis, Brownian motion and suction or injection effects [6]. Steady mixed convection boundary layer flow from an isothermal horizontal circular cylinder embedded in a porous medium filled with a nanofluid has been numerically studied for both the cases of a heated and cooled cylinder [7]. Steady mixed convection boundary layer flow of an incompressible nanofluid along a plate inclined at an angle α in a porous medium [8] has been analyzed. The problem of steady, laminar, mixed convection boundary-layer flow over an isothermal vertical wedge embedded in a porous medium saturated with a nanofluid in the presence of thermal radiation, has been numerically investigated [9] and they showed that, the effects of the radiation–conduction parameter and the surface temperature parameter are significantly stronger on the local Nusselt number than that on the local Sherwood number. The influence of the Soret effect on mixed convection heat and mass transfer in the boundary layer region of a semi-infinite vertical flat plate in a nanofluid has been presented under the convective boundary conditions [10] and they concluded that, the Soret effect enhanced the skin friction, heat, nanoparticle mass and regular mass transfer rates in the medium. The flow and radiation heat transfer of a nanofluid over a stretching sheet with velocity slip and temperature jump in porous medium has been solved both numerically and analytically by local similarity [11].

Previous studies on convection transport focussed on seeking similarity solution because, similar variables can give great physical insight with minimal effort. Most of the convection flows do not necessarily admit similarity solutions in many practical situations. Due to mathematical complexity involved in obtaining non-similar solutions for such problems, most researchers have confined their studies to similar flows. However, the non-similarity boundary layer flows are more general in nature in our everyday life, and thus are more important than the similarity ones. Hence, the aim of the present study is to obtain non-similar solutions and to study the effect of Brownian motion, Thermophoresis and Radiation on mixed convection heat and mass transfer over a vertical plate in a nanofluid saturated porous medium. The governing system of nonlinear partial differential equations is solved numerically using implicit finite difference method. The influence of pertinent parameters on the flow characteristics are examined and exhibited through graphs.

MATHEMATICAL FORMULATION

Consider the mixed convection boundary layer flow past a semi-infinite vertical flat plate embedded in a porous medium saturated with a nanofluid. Choose the coordinate system such that the x coordinate is along the plate, in the ascending direction and the y coordinate is normal to the plate, while the origin of the reference system is considered at the leading edge of the vertical plate. The plate has the constant wall heat, mass and nanoparticle fluxes. The porous medium is assumed to be uniform and isotropic and is in local thermal equilibrium with the fluid. The effects of Brownian motion and thermophoresis are incorporated into the model for nanofluids. The fluid properties are assumed to be constant except for density variations in the buoyancy force term.

Using the Boussinesq and boundary layer approximations, the governing equations for the conservation of total mass, momentum, energy and nanoparticles within the boundary layer near the vertical plate can be written as:

$$\frac{\partial u}{\partial x}+\frac{\partial v}{\partial y}=0 \qquad (1)$$

$$\rho_f\left(u\frac{\partial u}{\partial x}+v\frac{\partial u}{\partial y}\right)=\mu\frac{\partial^2 u}{\partial y^2}+(1-\phi_\infty)\rho_{f_\infty}g^*(\beta_T(T-T_\infty)$$

$$+\beta_C(C-C_\infty))-(\rho_p-\rho_{f_\infty})g^*(\phi-\phi_\infty)+\frac{\mu}{K_p}(u_\infty-u) \tag{2}$$

$$u\frac{\partial T}{\partial x}+v\frac{\partial T}{\partial y}=\alpha\frac{\partial^2 T}{\partial y^2}+\tau\left[D_B\frac{\partial\phi}{\partial y}\frac{\partial T}{\partial y}+\frac{D_T}{T_\infty}\left(\frac{\partial T}{\partial y}\right)^2\right]$$

$$+D_{TC}\frac{\partial^2 C}{\partial y^2}-\frac{1}{\rho C_p}\frac{\partial q_r}{\partial y} \tag{3}$$

$$u\frac{\partial C}{\partial x}+v\frac{\partial C}{\partial y}=D_s\frac{\partial^2 C}{\partial y^2}+D_{CT}\frac{\partial^2 T}{\partial y^2} \tag{4}$$

$$u\frac{\partial\phi}{\partial x}+v\frac{\partial\phi}{\partial y}=D_B\frac{\partial^2\phi}{\partial y^2}+\frac{D_T}{T_\infty}\frac{\partial^2 T}{\partial y^2} \tag{5}$$

The boundary conditions are:

$$u=0, v=0, q_w=-k\left(\frac{\partial T}{\partial y}\right)_{y=0}, q_m=-D_s\left(\frac{\partial C}{\partial y}\right)_{y=0},$$

$$q_{np}=-D_B\left(\frac{\partial\phi}{\partial y}\right)_{y=0} \quad \text{at } y=0 \tag{6a}$$

$$u\to u_\infty,\ T\to T_\infty,\ C\to C_\infty,\ \phi\to\phi_\infty \text{ as } y\to\infty \tag{6b}$$

Where the subscripts w and ∞ indicate the conditions at wall and at the outer edge of the boundary layer, respectively.

The radiative heat flux q_r is described by the Rosseland approximation such that

$$q_r=-\frac{4\sigma^*}{3k^*}\frac{\partial T^4}{dy} \tag{7}$$

We assume that the differences of the temperature within the flow are sufficiently small such that T^4 may be expressed as a linear function of the temperature. This is accomplished by expanding in a Taylor series about and neglecting higher-order terms, thus

$$T^4\cong 4T_\infty{}^3T-3T_\infty{}^4 \tag{8}$$

Making use of Eqs. (7) and (8) in the last term of Eqn. (3), we get

$$u\frac{\partial T}{\partial x}+v\frac{\partial T}{\partial y}=\alpha\frac{\partial^2 T}{\partial y^2}+\tau\left[D_B\frac{\partial\phi}{\partial y}\frac{\partial T}{\partial y}+\frac{D_T}{T_\infty}\left(\frac{\partial T}{\partial y}\right)^2\right]$$

$$+D_{TC}\frac{\partial^2 C}{\partial y^2}+\frac{16\sigma^*T_\infty{}^3}{3\rho C_p k^*}\frac{\partial^2 T}{\partial y^2} \tag{9}$$

The continuity equation (1) is satisfied by introducing the stream function ψ such that

$$u=\frac{\partial\psi}{\partial y},\ v=-\frac{\partial\psi}{\partial x} \tag{10}$$

Introducing the following non-dimensional variables

$$\left.\begin{aligned}\xi&=\frac{x}{L},\ \eta=\frac{Re^{1/2}}{L\xi^{1/2}}y,\ \psi=Re^{-1/2}\xi^{1/2}Lu_\infty f(\xi,\eta)`\\ T-T_\infty&=\frac{q_wL}{kRe^{1/2}}\xi^{1/2}\theta(\xi,\eta)\\ C-C_\infty&=\frac{q_mL}{D_sRe^{1/2}}\xi^{1/2}s(\xi,\eta)\\ \phi-\phi_\infty&=\frac{q_{np}L}{D_BRe^{1/2}}\xi^{1/2}g(\xi,\eta)\end{aligned}\right\} \tag{11}$$

Substituting Eqn. (11) into Eqs. (2), (4) - (5) and (9) we obtain

$$f'''+\frac{1}{2}ff''+\frac{\xi}{DaRe}(1-f')+Ri\xi^{3/2}(\theta+Bs-N_rg)$$

$$=\xi\left[f'\frac{\partial f'}{\partial\xi}-f''\frac{\partial f}{\partial\xi}\right] \tag{12}$$

$$\frac{1}{Pr}\left((1+\frac{4}{3}R)\theta''+N_b\xi^{1/2}g'\theta'+N_t\xi^{1/2}(\theta')^2+N_ds''\right)$$

$$+\frac{1}{2}f\theta'-\frac{1}{2}f'\theta=\xi\left[f'\frac{\partial\theta}{\partial\xi}-\theta'\frac{\partial f}{\partial\xi}\right] \tag{13}$$

$$\frac{1}{Sc}\left(s''+L_d\theta''\right)+\frac{1}{2}fs'-\frac{1}{2}f's=\xi\left[f'\frac{\partial s}{\partial\xi}-s'\frac{\partial f}{\partial\xi}\right] \tag{14}$$

$$\frac{1}{Sc_n}\left(g''+\frac{N_t}{N_b}\theta''\right)+\frac{1}{2}fg'-\frac{1}{2}f'g=\xi\left[f'\frac{\partial g}{\partial\xi}-g'\frac{\partial f}{\partial\xi}\right] \tag{15}$$

where the prime denote differentiation with respect to the similarity variable η, $B=\frac{\beta_C q_m k}{\beta_T q_w D_s}$ is the regular double diffusive buoyancy ratio, $N_r=\frac{(\rho_p-\rho_{f_\infty})q_{np}k}{\rho_{f_\infty}\beta_T(1-\phi_\infty)q_wD_B}$ is nanofluid buoyancy ratio, K_p is Permeability, $Da=\frac{K_p}{L^2}$ is Darcian number, $Ri=\frac{Gr}{Re^{5/2}}$ is mixed convection parameter, $Pr=\frac{\nu}{\alpha}$ is the Prandtl number,

$Gr = \dfrac{(1-\phi_\infty)\rho_{f_\infty} g^* \beta_T q_w L^4}{\mu \nu k}$ is Grashof number, $Sc = \dfrac{\nu}{D_s}$ is the Schmidt number, $N_t = \dfrac{\tau D_T q_w L}{\alpha T_\infty k Re^{1/2}}$ is thermophoresis parameter, $N_b = \dfrac{\tau q_{np} L}{\alpha Re^{1/2}}$ is Brownian motion parameter, $R = \dfrac{4\sigma^* T_\infty^{\,3}}{k k^*}$ is the radiation parameter, $Re = \dfrac{u_\infty L}{\nu}$ is Reynolds number, $Sc_n = \dfrac{\nu}{D_B}$ is nanofluid Schmidt number, $L_d = \dfrac{D_{CT} q_w}{q_m k}$ is Dufour-solutal Lewis number and $N_d = \dfrac{D_{TC} q_m k}{\alpha D_s q_w}$ is modified Dufour number.

The corresponding boundary conditions in dimensionless form are

$$f'(\xi,0)=0,\ f(\xi,0)+2\xi\left(\frac{\partial f}{\partial \xi}\right)_{\eta=0}=0,\ \theta'(\xi,0)=-1,$$
$$s'(\xi,0)=-1,\ g'(\xi,0)=-1 \tag{16a}$$

$$f'(\xi,\infty)=1,\quad \theta(\xi,\infty)=0,\quad s(\xi,\infty)=0,\quad g(\xi,\infty)=0 \tag{16b}$$

The heat, mass and nanoparticle volume fraction transfers from the plate respectively are given by

$$q_w=-k\left(\frac{\partial T}{\partial y}\right)_{y=0},\quad q_m=-D_s\left[\frac{\partial C}{\partial y}\right]_{y=0}$$
$$\text{and}\quad q_{np}=-D_B\left[\frac{\partial \phi}{\partial y}\right]_{y=0} \tag{17}$$

The non dimensional rate of heat-transfer, called the Nusselt number $Nu_\xi = \dfrac{q_w x}{k(T_w - T_\infty)}$, rate of mass transfer, called the Sherwood number $Sh_\xi = \dfrac{q_m x}{D_s(C_w - C_\infty)}$ and nanoparticle volume fraction transfer, called nanofluid Sherwood number $Sh_{n,\xi} = \dfrac{q_{np} x}{D_B(\phi_w - \phi_\infty)}$ are given by

$$\frac{Nu_\xi}{Re^{1/2}} = \frac{\xi^{1/2}}{\theta(\xi,0)},\quad \frac{Sh_\xi}{Re^{1/2}} = \frac{\xi^{1/2}}{s(\xi,0)} \text{ and}$$

$$\frac{Sh_{n,\xi}}{Re^{1/2}} = \frac{\xi^{1/2}}{g(\xi,0)} \tag{18}$$

RESULTS AND DISCUSSION

The governing nonlinear and non-homogeneous partial differential equations (12) - (15), are solved using very efficient implicit finite-difference scheme known as Keller-box method [12]. In the present study, the boundary conditions for η at ∞ are replaced by a sufficiently large value where the velocity, temperature and concentration approach zero. In order to see the effects of step size (Δη) we ran the code for our model with three different step sizes as Δη =0.001, 0.01 and 0.05 and in each case we found very good agreement between them on different profiles. After some trials we imposed a maximal value of η at ∞ of 8 and a grid size of Δη as 0.01.

In order to assess the accuracy of our method, we have compared our results with those of [13] in the absence of ξ, N_r, N_b, N_t, R, L_d and N_d with the variation of Prandtl number Pr. The comparison in the above case is found to be in good agreement, as shown in Table (1).

Table 1 Comparison between 1/θ(0) calculated by the present method and that of Lee et al.[13] with the variation of Prandtl number *Pr*

	1/θ(0)	
Pr	Lee et al.[13]	Present method
0.1	0.2007	0.20069
0.7	0.4059	0.4059
7	0.8856	0.88564
100	2.1512	2.15222

The effect of the thermophoresis N_t on velocity, temperature, concentration and nanoparticle volume fraction distributions is illustrated in Figures (1)-(4). It is noticed that the momentum boundary layer thickness enhances with the hike of N_t as depicted in Figure (1). An increase in N_t, causes a significant enhancement in temperature in the boundary layer as portrayed in Figure (2). Because, the thermophoresis force, which tends to move particles from the hot zone to the cold zone, increases with the rise in N_t. An increment in N_t diminishes the concentration near the plate and slightly enhances away from the plate as shown in Figure (3). Figure (4) illustrates that, the nanoparticle volume fraction is enhanced with the rising value of N_t.

Figures (5)-(8) demonstrates the effect of Brownian motion N_b on the velocity, temperature, concentration and nanoparticle volume fraction distributions. From Figure (5), we see that, the momentum boundary layer is strengthened with the increase of N_b. Figure (6) reveals that as the value of the Brownian motion parameter N_b increases the temperature of the fluid in the boundary layer increases. Because, the diffusion of nanoparticles into the fluid increases with the rise in N_b and thereby, the temperature profiles are enhanced. From Figure (7), we notice that, an increment in N_b reduces the concentration near the plate and slightly increases away from the plate. Figure (8) show that, the nanoparticle volume fraction is reduced with the increase of Brownian motion parameter N_b.

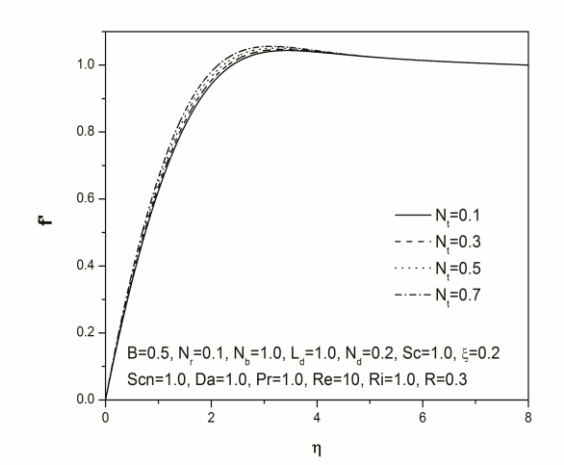

Figure 1 Velocity profiles for various values N_t

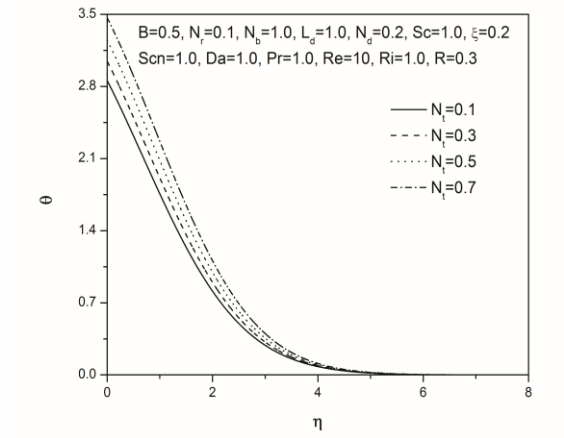

Figure 2 Temperature profiles for various values of N_t

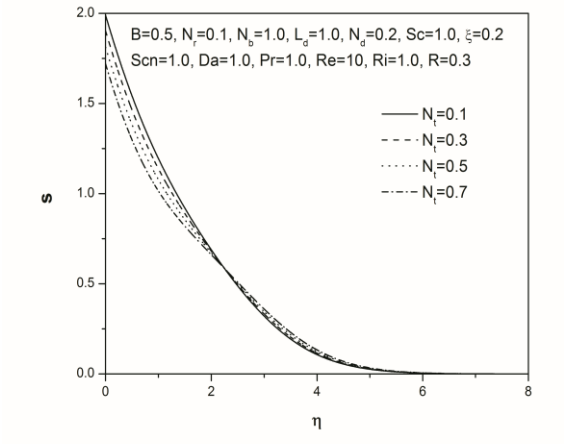

Figure 3 Concentration profiles for various values of N_t

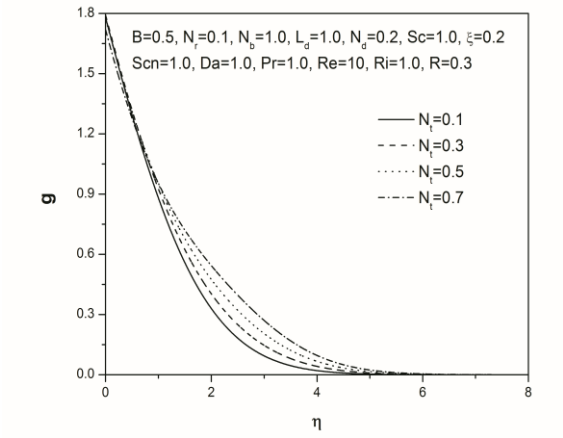

Figure 4 Nanoparticle volume fraction profiles for various values of N_t

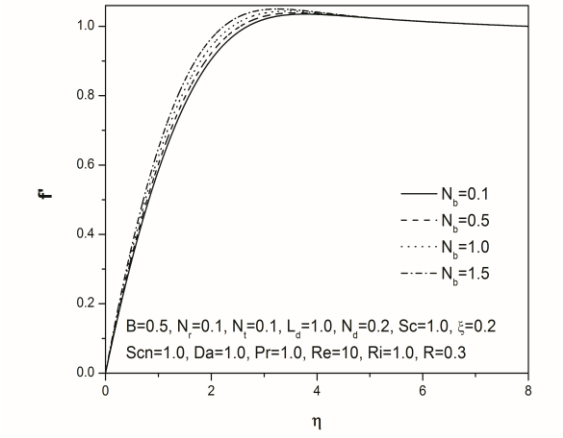

Figure 5 Velocity profiles for various values N_b

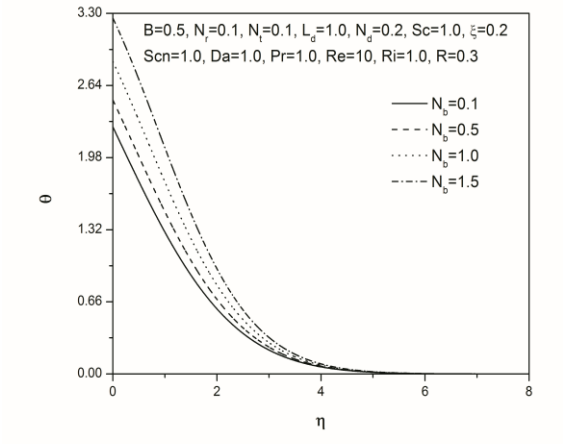

Figure 6 Temperature profiles for various values of N_b

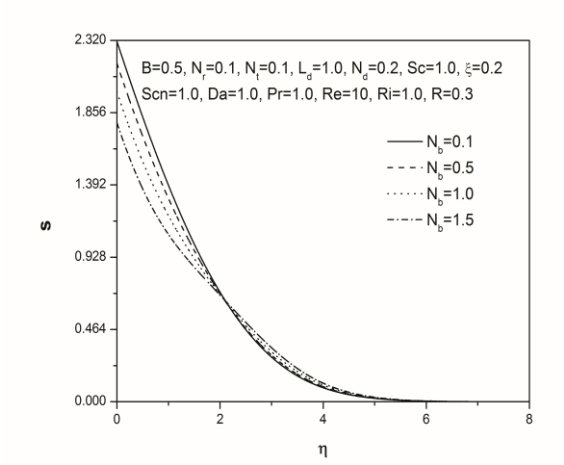

Figure 7 Concentration profiles for various values of N_b

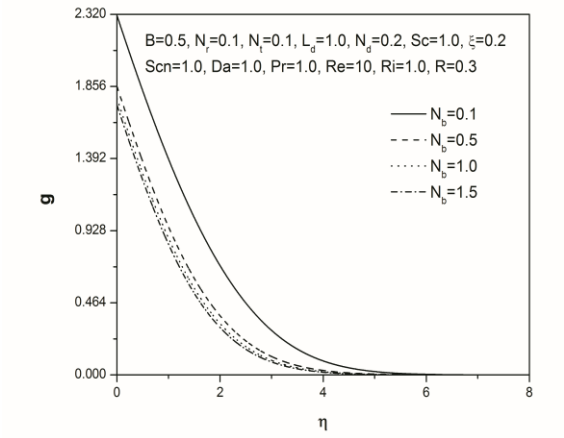

Figure 8 Nanoparticle volume fraction profiles for various values of N_b

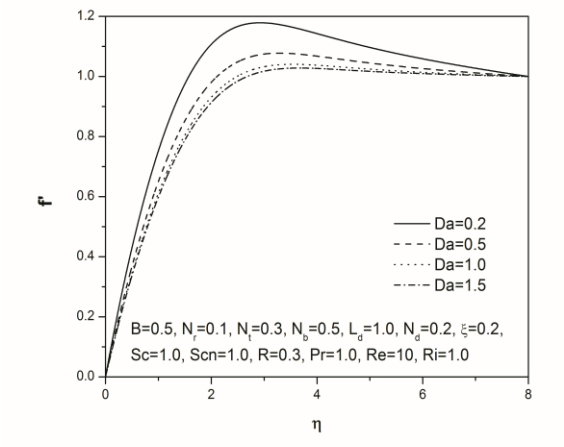

Figure 9 Velocity profiles for various values of *Da*

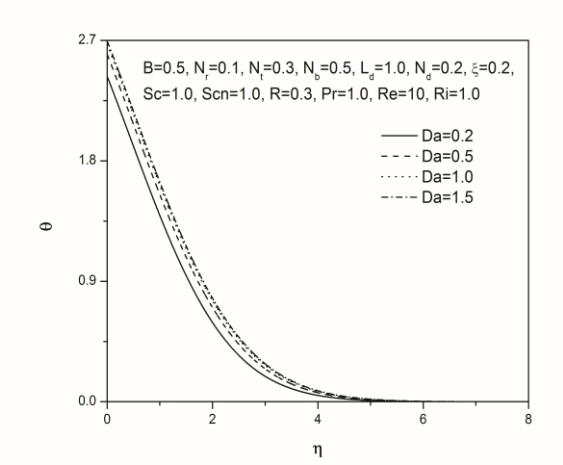

Figure 10 Temperature profiles for various values of *Da*

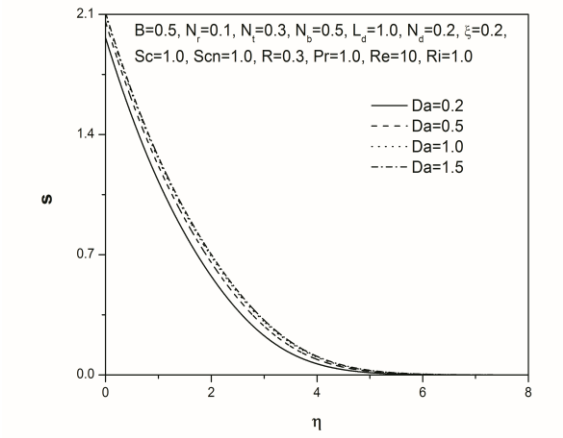

Figure 11 Concentration profiles for various values of *Da*

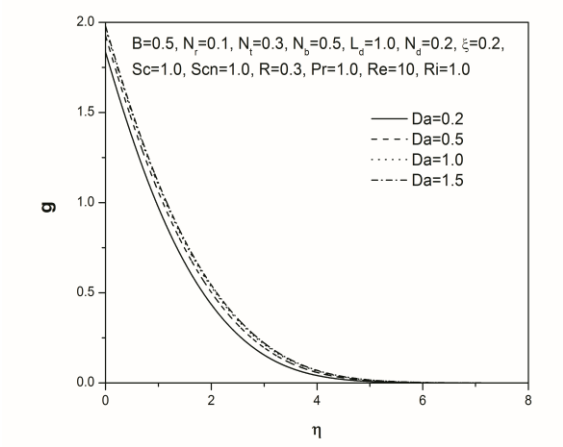

Figure 12 Nanoparticle volume fraction profiles for various values of *Da*

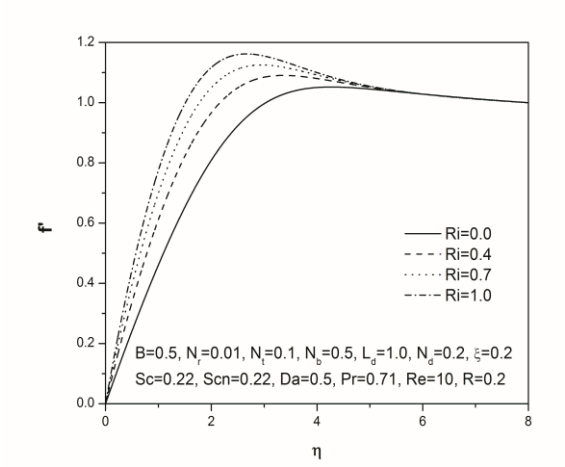

Figure 13 Velocity profiles for various values of *Ri*

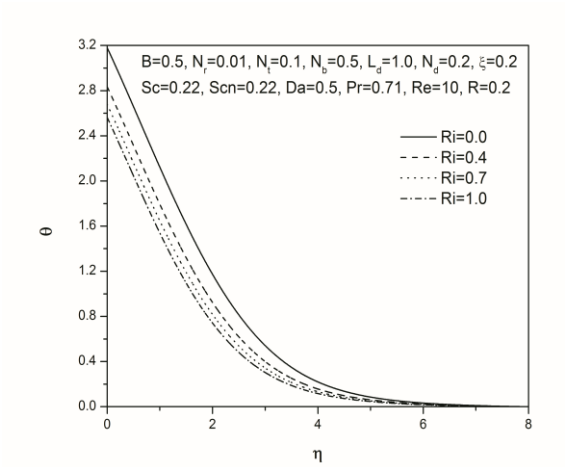

Figure 14 Temperature profiles for various values of *Ri*

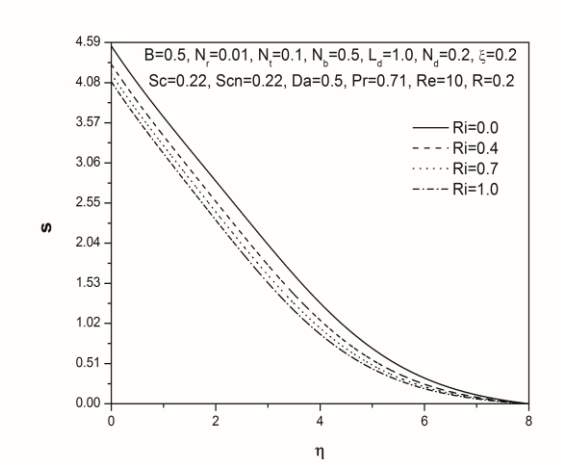

Figure 15 Concentration profiles for various values of *Ri*

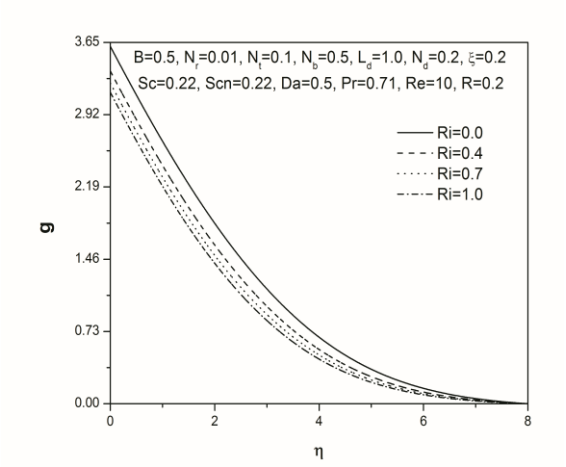

Figure 16 Nanoparticle volume fraction profiles for various values of *Ri*

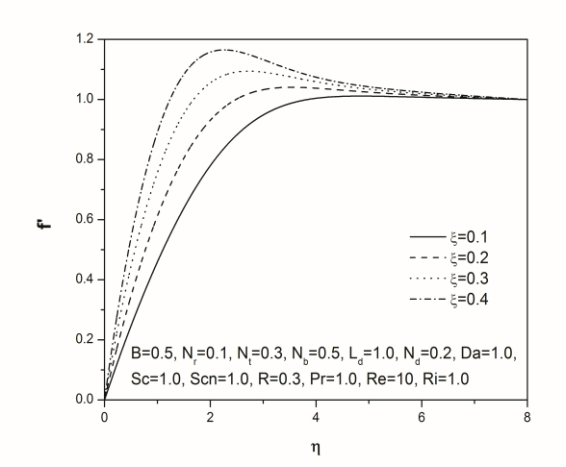

Figure 17 Velocity profiles for various values of ξ

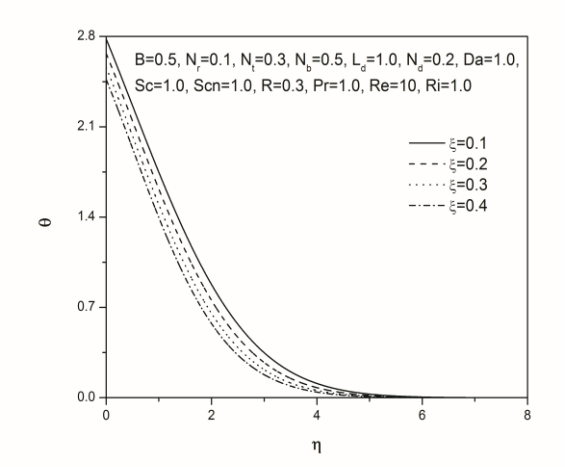

Figure 18 Temperature profiles for various values of ξ

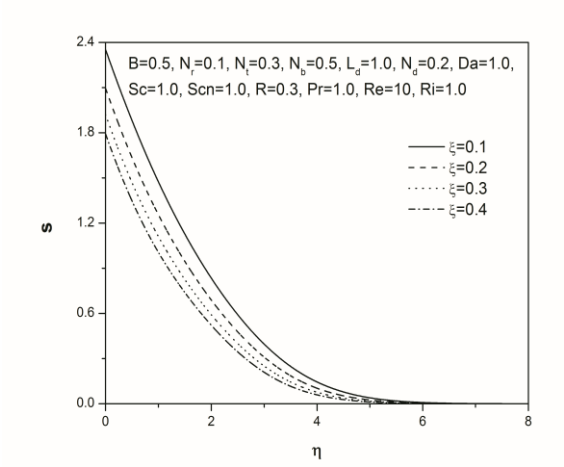

Figure 19 Concentration profiles for various values of ξ

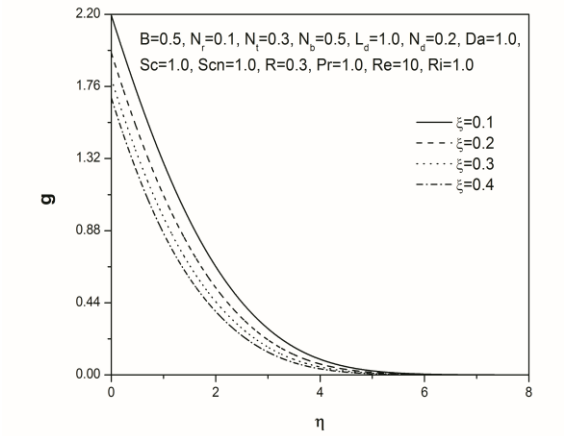

Figure 20 Nanoparticle volume fraction profiles for various values of ξ

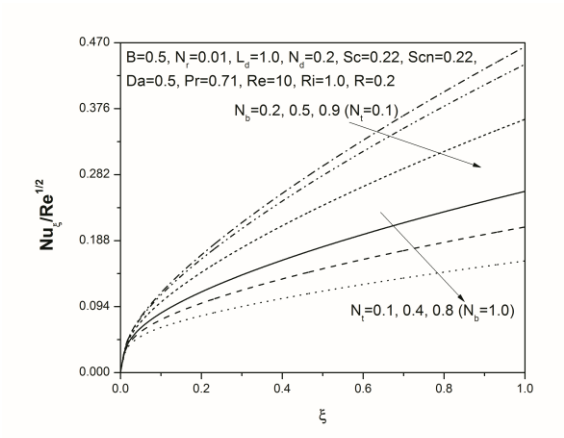

Figure 21 Variation of local heat transfer coefficient with N_t and N_b

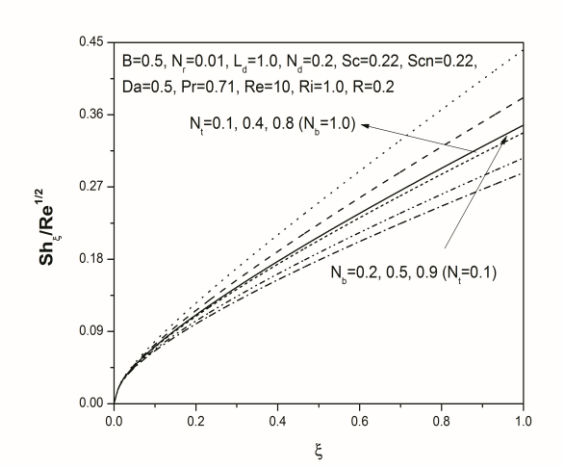

Figure 22 Variation of local mass transfer coefficient with N_t *and* N_b

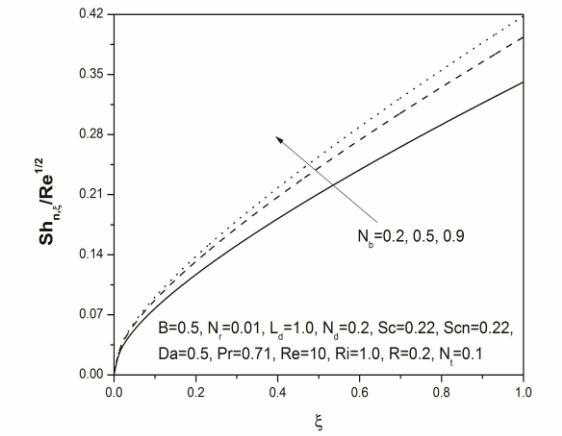

Figure 23 Variation of local nanoparticle transfer coefficient with N_t and N_b

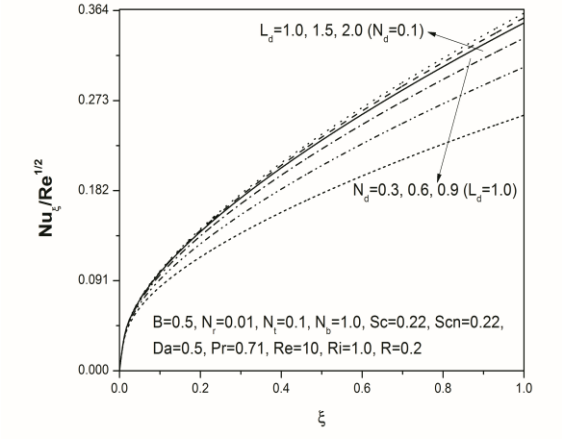

Figure 24 Variation of local heat transfer coefficient with L_d and N_d

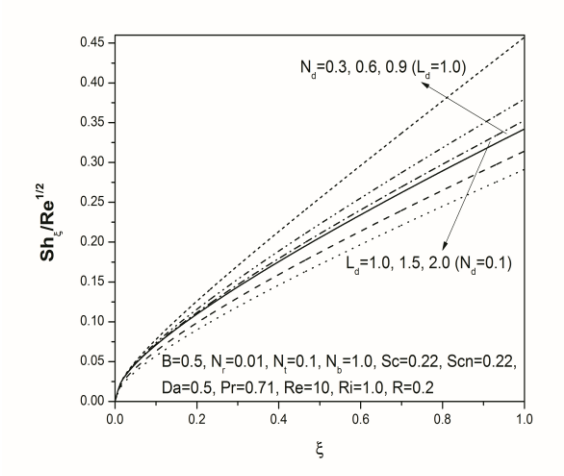

Figure 25 Variation of local mass transfer coefficient with L_d and N_d

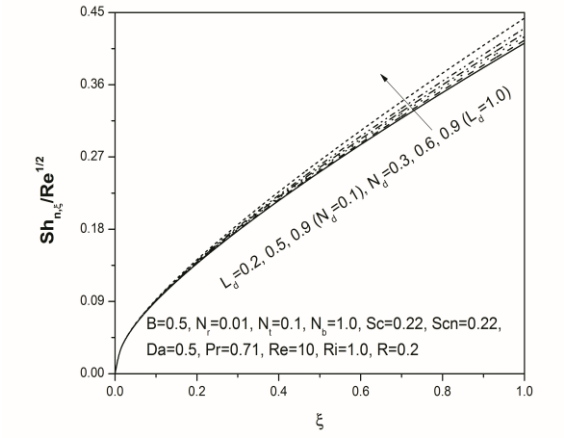

Figure 26 Variation of local nanoparticle transfer coefficient with L_d and N_d

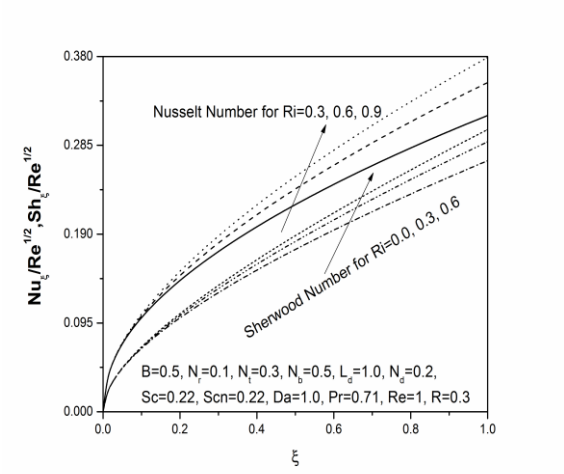

Figure 27 Variation of local heat and mass transfer coefficients with *Ri*

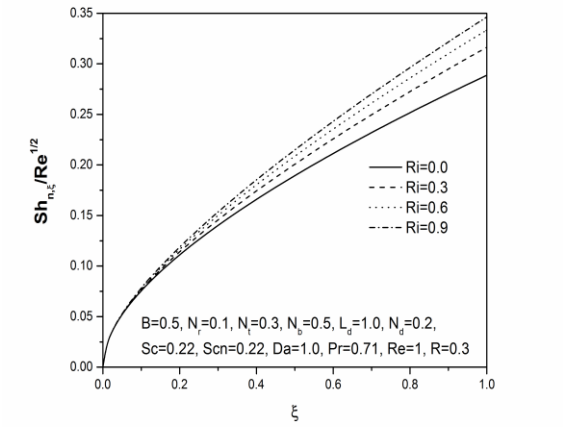

Figure 28 Variation of local nanoparticle transfer coefficient with *Ri*

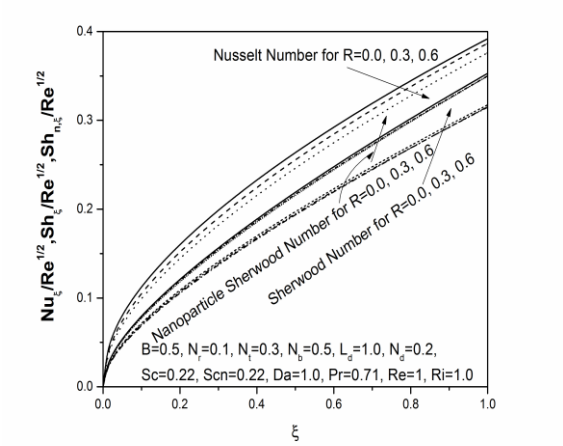

Figure 29 Variation of local heat, mass and nanoparticle transfer coefficients with *R*

The variation of velocity, temperature, concentration and nanoparticle volume fraction distributions with the variation of Darcy number is shown in Figures (9)-(12). Figure (9) reveals that, an increase in the Darcy number *Da*, reduces the intensity of the flow. The temperature of the fluid in the boundary layer is enhanced with the rise of *Da* as depicted in Figure (10). As the fluid is decelerated, energy dissipates as heat and it serves to enhance temperature in the boundary layer. Figures (11) and (12) show that, concentration and nanoparticle volume fraction boundary layers are strengthened with the rise of Darcy number *Da*.

The variation of non-dimensional velocity, temperature, concentration and volume fraction distributions with increasing mixed convection parameter is presented in Figures (13)-(16). As the mixed convection parameter *Ri* rise, the velocity increased whereas temperature, concentration and volume fraction of the nanofluid decreased. The influence of non-similarity variable ξ on velocity, temperature, concentration and

nanoparticle volume fraction is depicted in Figures (17)-(20). The momentum boundary layer is significantly increased with increasing value of non-similarity variable ξ where as the opposite trend is observed in the case of temperature, concentration and nanoparticle volume fraction. Thus an increase in ξ, reduced the temperature, concentration and nanoparticle volume fraction in the boundary layer.

The dimensionless heat, mass and nanoparticle mass transfer rates against ξ for different values of thermophoresis parameter N_t and Brownian motion parameter N_b are presented in Figures (21)-(23). Figure (21) depicts that the dimensionless heat transfer rate diminishes with the rise in both the thermophoresis and Brownian motion parameters. The dimensionless mass transfer rate enhance with the hike of both the thermophoresis and Brownian motion parameters, as shown in Figure (22). Increasing Brownian motion parameter enhances the nanoparticle mass transfer rate, as shown in Figure (23). The influence of thermophoresis parameter on nanoparticle mass transfer rate is not so significant and hence the graph is not included.

The variation of dimensionless Nusselt, Sherwood and nanoparticle Sherwood numbers for different values of Dufour-solutal Lewis number L_d and modified Dufour number N_d is exhibited in Figures (24)-(26). It is seen from Figure (24) that the dimensionless heat transfer rate is increased with the rise in the value of L_d and diminished with the increase of N_d. The dimensionless mass transfer rate enhances with the increase of modified Dufour number and reduced with an increasing value of Dufour-solutal Lewis number, as shown in Figure (25). Figure (26) reveals that, the nanoparticle mass transfer rate slightly increases with the hike in the values of both the Dufour-solutal Lewis number and modified Dufour number. Figures (27)-(28) presents the variation of non-dimensional Nusselt, Sherwood and nanoparticle Sherwood numbers with varying mixed convection parameter Ri. An increase in mixed convection parameter causes significant enhancement in dimensionless heat, mass and nanoparticle mass transfer rates. An increase in the radiation parameter R, significantly lessened the heat transfer rate and slightly enhanced the mass, nanoparticle mass transfer rates as shown in Figure (29)

CONCLUSION

In this article, the influence of thermophoresis, Brownian motion and radiation on mixed convection boundary layer flow of a nanofluid past a vertical plate embedded in a porous medium has been analyzed. The plate is subject to a uniform and constant wall heat, mass and nanoparticle fluxes. The main conclusions drawn from the present investigation are:

- An increase in thermophoresis parameter significantly enhanced the temperature, nanoparticle volume fraction and regular mass transfer rate but diminished the heat transfer rate in the boundary layer.
- The significance of Brownian motion parameter is to enhance velocity, temperature, and regular mass and nanoparticle mass transfer rates but to lessen nanoparticle volume fraction and heat transfer rate.
- The momentum boundary layer is diminished but the temperature, concentration and nanoparticle volume fraction are enhanced with the rise of Darcy number. Further, these quantities show an opposite trend with the increasing value of mixed convection parameter. The heat, regular mass and nanoparticle transfer rates are significantly increased with increasing value of mixed convection parameter.
- The influence of non-similarity variable on flow characteristics is much pronounced and the effect of radiation is to diminish the heat transfer rate in the boundary layer.

ACKNOWLEDGEMENTS

The authors would like to thank the DST, Govt. of India for providing travel support from ITS scheme to present this paper in the conference.

REFERENCES

[1] Choi, S.U.S., Zhang, Z.G., Yu, W., Lockwood, F.E., and Grulke, E.A., Anomalously thermal conductivity enhancement in nanotube suspension, *Applied. Physics Letters*, Vol. 79, 2001, pp. 2252-2254

[2] Das, S.K., Choi, S.U.S., Yu, W., and Pradeep, T., *Nanofluids: Science and Technology*, 2007, Wiley Interscience, New Jersey

[3] Buongiorno, J., Convective transport in nanofluids, *ASME Journal of Heat Transfer*, Vol. 128, 2006, 240-250

[4] Kakac, S., and Pramuanjaroenkij, A., Review of convective heat transfer enhancement with nanofluids, *International Journal of Heat and Mass Transfer*, Vol. 52, 2009, 3187-3196

[5] Gianluca, P., Samuel, P., and Sen, M., Nanofluids and their properties, *Applied Mechanics Reviews*, Vol. 64, 2011, Article number 030803

[6] Chamkha, A.J., Aly, A.M., and Al-Mudhaf, H.F., Laminar MHD mixed convection flow of a nanofluid along a stretching permeable surface in the presence of heat generation or absorption effects, *International Journal of Microscale and Nanoscale Thermal and Fluid Transport Phenomena*, Vol. 2, 2011, 51-70

[7] Nazar, R., Tham, L., Pop, I., and Ingham, D.B., Mixed convection boundary layer flow from a horizontal circular cylinder embedded in a porous medium filled with a nanofluid, *Transport in Porous Media*, Vol. 86, 2011, 517-536

[8] Rana, P., Bhargava, R., and Beg, O.A., Numerical solution for mixed convection boundary layer flow of a nanofluid along an inclined plate embedded in a porous medium, *Computers and Mathematics with Applications*, Vol. 64, 2012, 2816-2832

[9] Chamkha, A.J., Abbasbandy, S., Rashad, A.M., and Vajravelu, K., Radiation effects on mixed convection over a wedge embedded in a porous medium filled with a nanofluid, *Transport in Porous Media*, Vol. 91, 2012, 261-279

[10] RamReddy, Ch., Murthy, P.V.S.N., Chamkha, A,J., and Rashad, A.M., Soret effect on mixed convection flow in a nanofluid under convective boundary condition, *International Journal of Heat and Mass Transfer*, Vol. 64, 2013, 384-392

[11] Zheng, L., Zhang, C., Zhang, X., and Zhang, J., Flow and radiation heat transfer of a nanofluid over a stretching sheet with velocity slip and temperature jump in porous medium, *Journal of Franklin Institute*, Vol. 350, 2013, 990-1007

[12] Cebeci, T., and Bradshaw, P., *Physical and Computational Aspects of Convective Heat Transfer*, 1984, Springer Verlin

[13] Lee, S.L., Chen, T.S., and Armaly, B.F., Mixed convection along vertical cylinders and needles with uniform surface heat flux, *ASME Journal of Heat Transfer*, Vol. 109, 1987, 711-716